Stochastic Wind Forcing of Baroclinic Rossby Waves in the Presence of a Meridional Boundary

ANGELIKA LIPPERT AND ROLF H. KÄSE

Institut für Meereskunde an der Universität Kiel, Kiel, FRG

(Manuscript received 29 December 1983, in final form 23 November 1984)

ABSTRACT

The quasigeostrophic response of a continuously stratified ocean to a band-limited white-noise windstress curl is examined in an infinite and semi-infinite ocean. Baroclinic Rossby waves—predominantly of first mode character—determine an energy range in the frequency spectra as a result of the finite range of scales in the forcing and wave dispersion. Free waves emanating from an eastern boundary superimpose on resonantly excited waves and lead to a nonhomogeneous zonal distribution of energy which increases westward.

1. Introduction

Fluctuating windfields are a possible generating agent for mesoscale variability in the ocean. Early studies considered the windfield to be deterministic and calculated the ocean's response to a particular wind pattern, whereas the interest in stochastic forcing models increased in the last ten years. The classical paper by Veronis and Stommel (1956) describes the response of a two-layer, inviscid fluid by deterministic winds. It is shown that an oscillating windfield with periods ranging from one day to one year excites geostrophically balanced planetary Rossby waves of barotropic and baroclinic character, while in the long-period range ($\geq$100 years) the response is strongly baroclinic and confined to the upper layer. Since the windstress variations are to a large extent random fluctuations, models which account for the statistical nature of the response are required. The response of an infinite ocean to white-noise forcing in the frequency range of inertia-gravity waves was studied by Käse and Tang (1976). Magaard (1977) concentrated his studies to the planetary Rossby wave range. Stochastic forcing was also considered by Frankignoul and Müller (1979), Willebrand *et al.* (1980) and Müller and Frankignoul (1981), henceforth referred to as MF. MF presented an analytical quasi-geostrophic model involving a normal mode expansion in the vertical coordinate where dissipation processes were parameterized by Rayleigh damping.

They were able to construct a spectral model of the modal and depth-integrated energy in the range of barotropic and baroclinic Rossby waves. By applying the hypothetical windstress wavenumber spectrum of their earlier paper, MF produced results which are in agreement with the observations. However, the model implies that the high wavenumber cutoff of the forcing extends beyond the inverse Rossby radius of deformation, a fact which does not seem to be supported by Willebrand's analysis (1981).

The implications of a cutoff in the wavenumber space at a scale larger than the inverse Rossby radius would be of interest, as well as the modification of the resulting spectra due to the effects of horizontal boundaries. Since a linear model without horizontal boundaries cannot excite motion in a range of scales completely different from that of the forcing, a spectral cutoff at smaller wavenumbers results in a larger scale current field. The inclusion of a lateral boundary, however, leads to different results: A spatially uniform curl of the windstress which is variable in time generates Rossby waves at an eastern boundary (White, 1977). It is essentially the same process of generation as discussed by Anderson and Gill (1975) in their model of baroclinic spin-up of the gyre-circulation.

Most observations of baroclinic Rossby waves come from the Pacific Ocean. Kang and Magaard (1980) report first mode baroclinic Rossby waves at the annual frequency. The energy of these waves increases with distance from the coastline of North America. Mysak (1983) argues that this is a result of a localized forcing at a higher latitude.

Several studies show that an interpretation under two different basic assumptions concerning the nature of the wave field is possible. Price and Magaard (1983) assume that the wave field is composed of an ensemble of first mode Rossby waves with random amplitudes and phases, whereas White and Saur (1981) argue that the results of a harmonic analysis of the wave field with the annual period show a strong phase coupling in the vicinity of the eastern

boundary which is also indicated by a simple deterministic forcing model. Price and Magaard (1983) compare both methods and find that the deterministic phase coupling probably is better justified in the range of about 2000 km off the eastern coast, while in the midocean a fit with random phases yields better results. This suggests that a model for the North Atlantic must incorporate both mechanisms, since the range where deterministic phases are possibly dominant covers a considerable fraction of the ocean due to the smaller aspect ratio.

Several experiments were made in the Canary Basin within the framework of the "Warmwassersphäre"-Research Project. Käse *et al.* (1984) analysed current-meter records and density maps with respect to Rossby waves and found that the meridional component of the current velocity has an energy level which is 3–4 times larger than the zonal component (Fig. 1). The dominant period of the meridional flow is 138 days and does not differ so much from the hypothetical cutoff frequency of a linear Rossby wave model (~½ year) (Käse *et al.*, 1984).

In the present paper we attempt to explain some of the observed features of the flow by means of a simple linear forcing model that combines direct forcing by stochastic winds and effects of an eastern boundary.

2. Formulation

Fluctuations of the current and density field in the time range of baroclinic Rossby waves are usually described by the quasi-geostrophic vorticity equation (e.g., Veronis, 1981). Forcing by the atmosphere is treated in such a way that the convergent Ekman transport leads to an Ekman pumping velocity at the base of the upper boundary layer.

Thus the streamfunction is governed by

$$\frac{\partial}{\partial t}\left(\nabla^2 + \frac{\partial}{\partial z}\frac{f_0^2}{N^2}\frac{\partial}{\partial z}\right)\psi + \beta\frac{\partial\psi}{\partial x} = D. \tag{1}$$

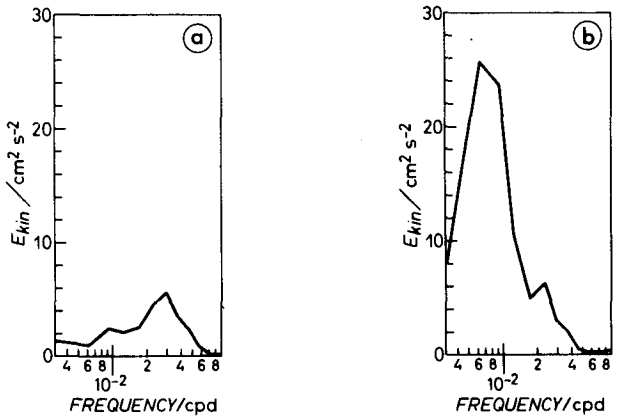

FIG. 1. Frequency spectra of zonal (a) and meridional (b) kinetic energy at 700 m depth of mooring NEADS 1 (ϕ = 33°N, λ = 22°W). Note the energy preserving form.

If we assume a free slip at the bottom and a rigid-lid condition at the surface, the boundary conditions are

$$\frac{\partial^2\psi}{\partial t\partial z} = \frac{N^2}{f_0^2}\,\mathrm{rot}_z\tau \quad \text{at} \quad z = 0, \tag{2}$$

$$\frac{\partial^2\psi}{\partial t\partial z} = 0 \quad \text{at} \quad z = H. \tag{3}$$

Here D includes all dissipation and nonlinear terms. To simplify the problem we project all effects into one term, similar to MF. Models which include barotropic and baroclinic motions have to face the problem of a parametrization that takes the different time and space scales of the motion into account. Müller and Frankignoul have used a combination of Rayleigh damping and Newtonian cooling resulting in a dissipation time of 200 days. Their special damping term forces an equi-partition of kinetic and potential energy, a fact which is not really observed at long time scales. Since we will restrict our attention to baroclinic waves only, we favour an eddy viscosity concept where D takes the form

$$D = \frac{\partial}{\partial z}\mu(z)\frac{\partial}{\partial z}\nabla^2\psi. \tag{4}$$

At an eastern boundary which is assumed to be a meridional wall the normal velocity has to vanish. Thus the condition in terms of the streamfunction reads

$$\frac{\partial\psi}{\partial y} = 0 \quad \text{at} \quad x = 0. \tag{5}$$

3. Infinite ocean

a. *Forced solution*

The solution of the problem is simplified considerably if we introduce a normal mode expansion in terms of the eigenfunctions Z_n which are solutions of the Sturm-Liouville problem

$$\frac{d^2W_n}{dz^2} + \lambda_n^2 N^2 W_n = 0 \tag{6}$$

with

$$W_n = 0 \quad \text{at} \quad z = 0, H. \tag{7}$$

Transforming (1) into Fourier space with respect to time and horizontal coordinates, we obtain the modal amplitudes by multiplying (1) with $dW_n/dz = Z_n$ and integrating by parts. A special distribution of the viscosity is chosen to further simplify the solution (Fjeldstad, 1964; McCreary, 1981a,b). This form makes the frictional modes compatible with the gravity modes resulting in a momentum flux divergence which has the same shape as the velocity profile. An equivalent depth dependence is also claimed by Broecker (1981) for the apparent tracer diffusivity.

The solution for the modal amplitudes results in

$$\psi_n = \mathrm{rot}_z \tau Z_n(z)Z_n(0)/[(k^2 + f_0^2\lambda_n^2)(\omega - \omega_n)], \quad (8)$$

$$\omega_n = \frac{\beta\kappa + ik^2\mu_0 N_0^2 \lambda_n^2}{k^2 + f_0^2\lambda_n^2}. \quad (9)$$

The character of the stochastic fluctuations induced by the windstress curl is described by the frequency wavenumber spectra

$$\Omega(\kappa, \eta, \omega, z) = F_{\mathrm{rot}} \cdot |\sum_{n=1}^{N} Z_n(0)Z_n(z) \cdot R(\kappa, \eta, \omega)|^2, \quad (10)$$

where F_{rot} is the spectrum of the windstress curl and $R(\kappa, \eta, \omega)$ is the transfer function of the system

$$R(\kappa, \eta, \omega) = \left\{ i\omega[k^2(1 + i\mu_0 N_0^2 \lambda_n^2/\omega) - \frac{\beta\kappa}{\omega} + f_0^2\lambda_n^2] \right\}^{-1} \quad (11)$$

with $k^2 = \kappa^2 + \eta^2$. It is noteworthy that in our formulation the individual modes are not statistically independent, thus (10) also contains mixed terms, which describe the contribution by interference of modes with a different mode number. These terms become increasingly important at periods longer than about 4 years, since more individual modes can be excited. However, if we restrict the discussion to depth integrated spectra, the coupling terms vanish due to the orthogonality condition. In that case the transfer function is identical to that used in MF except for the frictional term.

b. Dissipation

Models with stationary stochastic forcing require a dissipation mechanism in order to prevent infinite response at free wave resonance. This damping introduces an imaginary part in the dispersion relationship. In case of eddy viscosity parametrization this relationship is given by (9).

The real part is identical to the eigenfrequency of inviscid free Rossby waves. The imaginary part represents a decay rate and in our formulation is wavenumber dependent and directly proportional to the magnitude of the viscosity. Eddy coefficients have been used in various studies of different processes in fluid dynamics. Using this form of parametrization we design a damping that has some advantages. First, the high wavenumber components are much more diminished than the lower ones. Second, the higher modes are reduced. This is a feature often observed in the ocean, where the first baroclinic mode is strongly dominant (Magaard, 1983). Third, this damping leads to a ratio of total potential to kinetic energy larger than one. This is also an observable characteristic of the baroclinic Rossby wave field. Further, it makes our results directly comparable to other studies, in which a selective damping is used (e.g., Mysak and Magaard, 1983).

Figure 2 shows the wavenumber dependence of the relative damping defined as the ratio of the imaginary and real part of the first mode eigenfrequency for our damping (a) and the damping used by MF (b). The calculation in (a) used a damping $R = \mu_0 N_0^2 \lambda_1^2$, corresponding to 1.11×10^{-7} s^{-1}. This compares with a value of 5×10^{-8} s^{-1} used by Mysak and Magaard (1983). In the range of wavelengths between 300 and 3000 km the damping does not effect the wave propagation considerably. This is also evident in (b). Due to the normalization with frequency the isolines in case (b) correspond to resonance circles of the free waves. Thus, our dissipation has a considerably smaller effective damping in the range of long waves compared to MF. It will be shown later that in the case of a semi-infinite ocean, friction is not crucial in determining the character of the wave field.

c. Spectra of windstress curl

Evaluation of the energy spectra requires a detailed knowledge of the frequency wavenumber spectrum

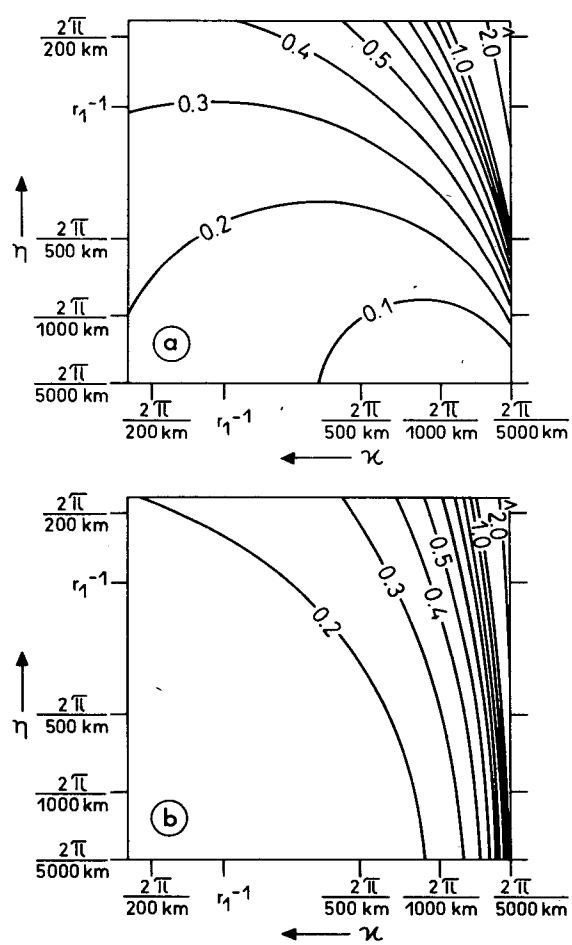

FIG. 2. Ratio of imaginary part to real part of resonant frequency with $R = 1.11 \times 10^{-7}$ s^{-1} for vertical eddy viscosity damping (a) and $R = 5 \times 10^{-8}$ s^{-1} for MF-damping (b).

of the curl of the windstress. MF use a hypothetical spectrum that yields the form

$$\Omega_{\mathrm{rot}\tau}(\mathbf{k}, \omega) = \frac{3}{4} F_\tau(0) \frac{k_b}{k} S(k) \qquad (12)$$

with $F_\tau(0) = 10^4 N^2$ m^{-4} s and

$$S(k) = \begin{cases} \dfrac{k^4}{k_b^4}, & 0 \leqslant k \leqslant k_b \\ 1, & k_b \leqslant k \leqslant k_c \\ 0, & k \geqslant k_c. \end{cases}$$

The white-noise level of the frequency spectrum of the windstress curl in MF is two orders of magnitude larger than that in Willebrand's (1981) analysis. This is the effect of contributions to the variance by small scale components which are not present in Willebrand's strongly smoothed data set. In the present analysis emphasis is not on the absolute value of the curl. Rather we are interested in the behaviour of the frequency spectrum in response to a different choice of the high wavenumber cut off. Our calculations are based on a white-noise level of 1.65×10^{-8} N^2 m^{-6} s corresponding to an rms curl of 10^{-7} N^2 m^{-6} in the range of periods larger than 120 days. For a higher rms-value the response can be calculated by multiplication.

d. Spectra of baroclinic Rossby waves

The shape of the frequency spectra strongly depends on the wavenumber bandwidth of the curl spectra. Since most of the response is generated resonantly, the response spectra reflect the signatures of the forcing via the dispersion relation. In case of a broad band according to MF the kinetic energy spectrum is essentially white at frequencies smaller than the cutoff frequency of the first baroclinic mode

$$\omega_c = \frac{\beta r_1}{2}, \qquad (13)$$

where r_1 is the first mode Rossby radius (41 km in our calculations).

At higher frequencies there is a falloff according to ω^{-2}. A different picture arises if the bandwidth is significantly smaller. Since it is not clear whether the plateau region in the curl wavenumber spectrum extends beyond the inverse Rossby radius, the following discussion puts emphasis on how varying the bandwidth affects the oceanic spectra. We calculated the kinetic energy spectra for several combinations of the parameters k_b and k_c.

To allow for an anisotropic distribution in wavenumber space we introduce cutoff wavenumbers of the zonal ($\kappa_{c,b}$) and the meridional ($\eta_{c,b}$) wavenumber component. The magnitudes of these cut-off wavenumbers are then k_c and k_b, respectively.

Figures 3 and 4 show the results which clarify the influence of varying k_b with k_c fixed (Fig. 3) and varying k_c with k_b fixed (Fig. 4). If k_b and k_c take the values according to MF, the baroclinic response is comparable (Fig. 3d), i.e., white noise. Changing the right cutoff to lower values shifts the falloff to lower frequencies if κ_c is smaller than r_1^{-1}. The dispersion curve as function of the zonal wavenumber bandwidth at small meridional wavenumbers (also shown in Fig. 3) determines the position of the cutoff.

The reduction of the bandwidth due to changes in k_b with fixed right cutoff k_c modifies the frequency spectrum from a broad band to a narrow band character (Fig. 4). This is mainly due to the left zonal cutoff at large meridional wavenumbers. The low frequency limit of first mode Rossby waves is determined by the resonance frequency for the largest zonal and the smallest meridional wavelength of the forcing. For a choice of $k_b = 2\pi/5000$ km and $k_c = 2\pi/500$ km the spectrum of kinetic energy shows a broad peak around the annual frequency with periods between ½ and 4 years. This is also the range where Magaard (1983) reports on most of the potential energy of Rossby waves in the eastern Pacific. We shall attend to this fact later when the influence of

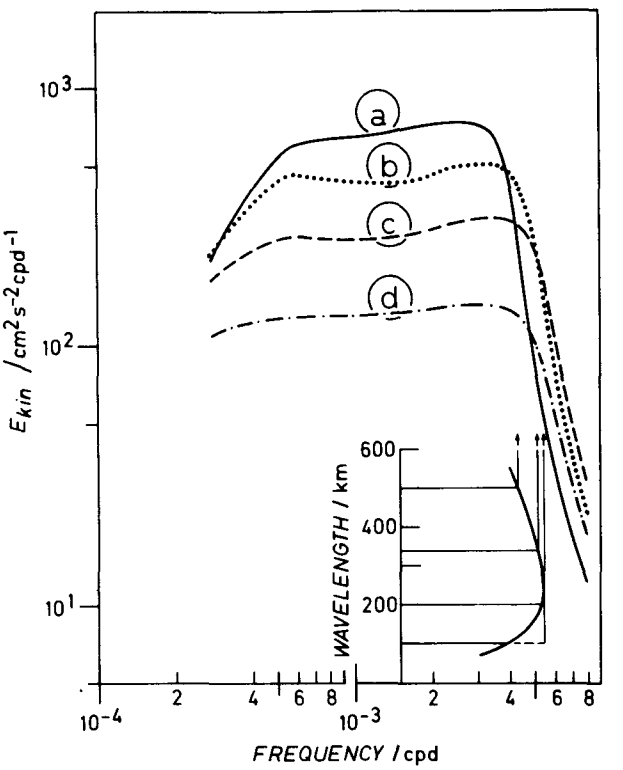

FIG. 3. Kinetic energy spectra of first mode baroclinic Rossby waves resulting from different wavenumber bands of the windstress curl. Dispersion relation $\omega = \beta\kappa_c/(\kappa_c^2 + \eta_b^2 + r_1^{-2})$, which determines the upper limit of the resonant range in the lower right. The upper limit $\kappa_c = \eta_c$ is (a) $2\pi/500$ km; (b) $2\pi/333$ km; (c) $2\pi/200$ km; (d) $2\pi/100$ km; the lower limit $\kappa_b = \eta_b = 2\pi/5000$ km.

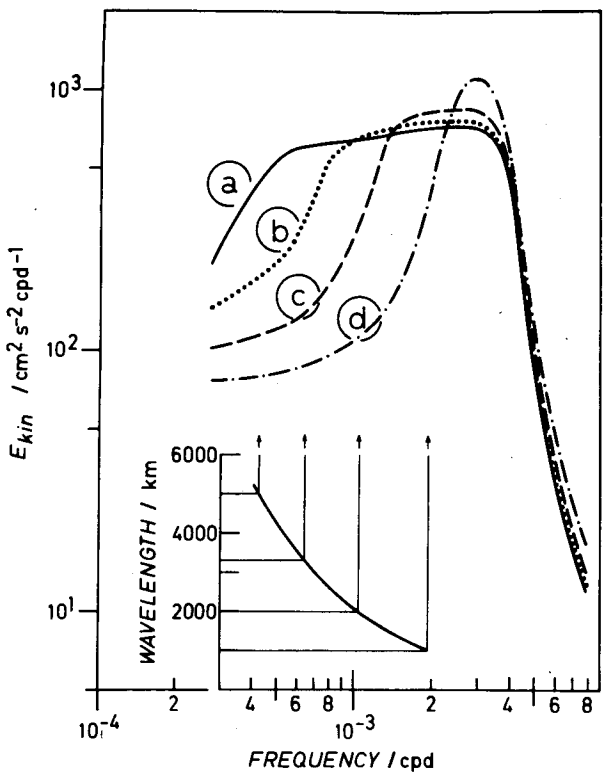

FIG. 4. Kinetic energy spectra of first mode baroclinic Rossby waves resulting from different wavenumber bands of the windstress curl (top). Dispersion relation $\omega = \beta\kappa_b/(\kappa_b^2 + \eta_c^2 + r_1^{-2})$, which determines the lower limit of the resonant range (bottom). The lower limit $\kappa_b = \eta_b$ is (a) $2\pi/5000$ km; (b) $2\pi/3333$ km; (c) $2\pi/2000$ km; (d) $2\pi/1000$ km; The upper limit $\kappa_c = \eta_c = 2\pi/500$ km.

coastal forcing will be considered in combination with the direct response.

Since the measurements of current fluctuations in the eastern North Atlantic reveal a significantly higher energy level in the meridional component, we tried to take account of this fact by using a slight anisotropic forcing. The dominance of meridional energy suggests that the zonal wavenumbers of the curl should be more energetic in the case of direct wind forcing. Figure 5 displays in an energy preserving form the variance spectra of the zonal (solid line) and meridional component (dashed line) of current velocity at 100 m depth. Figures 5a and 5b were produced by an isotropic curl spectrum with a broad band (a) and a narrow band (b). Both components have approximately the same total variance but it is distributed differently in frequency. Figures 5c and 5d exhibit a higher (smaller) level in the meridional component due to a broad (narrow) zonal wavenumber band of the curl spectrum. Concerning the meridional-component case, (b) and (c) show agreement with the observations in the Canary Basin. Further interpretation of the observations in terms of the forcing is, however, not advisable since the vicinity of the eastern boundary imposes some constraints on the general validity of the theory of directly forced response. In the next chapter we include the influence of a simple meridional eastern boundary and show that the coastal forcing further broadens the scope of interpretation of the observed features.

4. Semi-infinite ocean

a. Including an eastern boundary

White's (1977) analysis of baroclinic Rossby waves at the annual period showed that baroclinic Rossby waves can be generated by a simple time varying windstress curl if an eastern boundary is introduced. The solution was given for a two-layer model in which the forced response at the coast is compensated by nondispersive baroclinic Rossby waves; their amplitudes are therefore determined by the condition which is imposed by the eastern boundary. Krauss and Wübber (1981) calculated the response to a spatially varying windstress curl in a closed rectangular basin fulfilling the boundary conditions by compensating the directly forced waves by free waves.

In order to account for the stochastic nature of the wind field we introduce random phases for the individual Fourier components. The boundary condition (5) requires that each realization of the directly forced response, defined as the integral over all wavenumbers, must be balanced by westward propagating free Rossby waves. This requires that

$$\sum_{\omega'}\sum_{\eta'}\sum_{n=1}^{\infty} A_n Z_n e^{i\omega' t + i\eta' y} = -\sum_{\omega}\sum_{\eta}\sum_{\kappa}\sum_{n=1}^{\infty} F_n Z_n e^{i\phi_\kappa + i\omega t + i\eta y + i\phi_\eta + i\phi_\omega} \quad (14)$$

holds, where A_n are the amplitudes of the free waves and F_n those of the forced waves, respectively. ϕ_κ, ϕ_η, ϕ_ω are random phases.

The unknown amplitudes A_n are thus given by

$$A_n(\omega, \eta) = e^{i\phi_\eta + i\phi_\omega} \sum_{\kappa} F_n e^{i\phi_\kappa}, \quad (15)$$

and the total solution reads

$$\psi(\eta, \omega, z, x) = \sum_{\kappa}\sum_{n=1}^{\infty} F_n Z_n e^{i\phi_\kappa + i\kappa x} - \sum_{n=1}^{\infty} Z_n e^{i\kappa_n x} \sum_{\kappa} F_n e^{i\phi_\kappa}. \quad (16)$$

The frequency meridional wavenumber spectrum of the streamfunction is obtained by multiplying (16) with its complex conjugate and subsequent ensemble averaging.

If we integrate over the depth range, the modal coupling term vanishes and the spectra of potential energy and of zonal and meridional kinetic energy take the following form

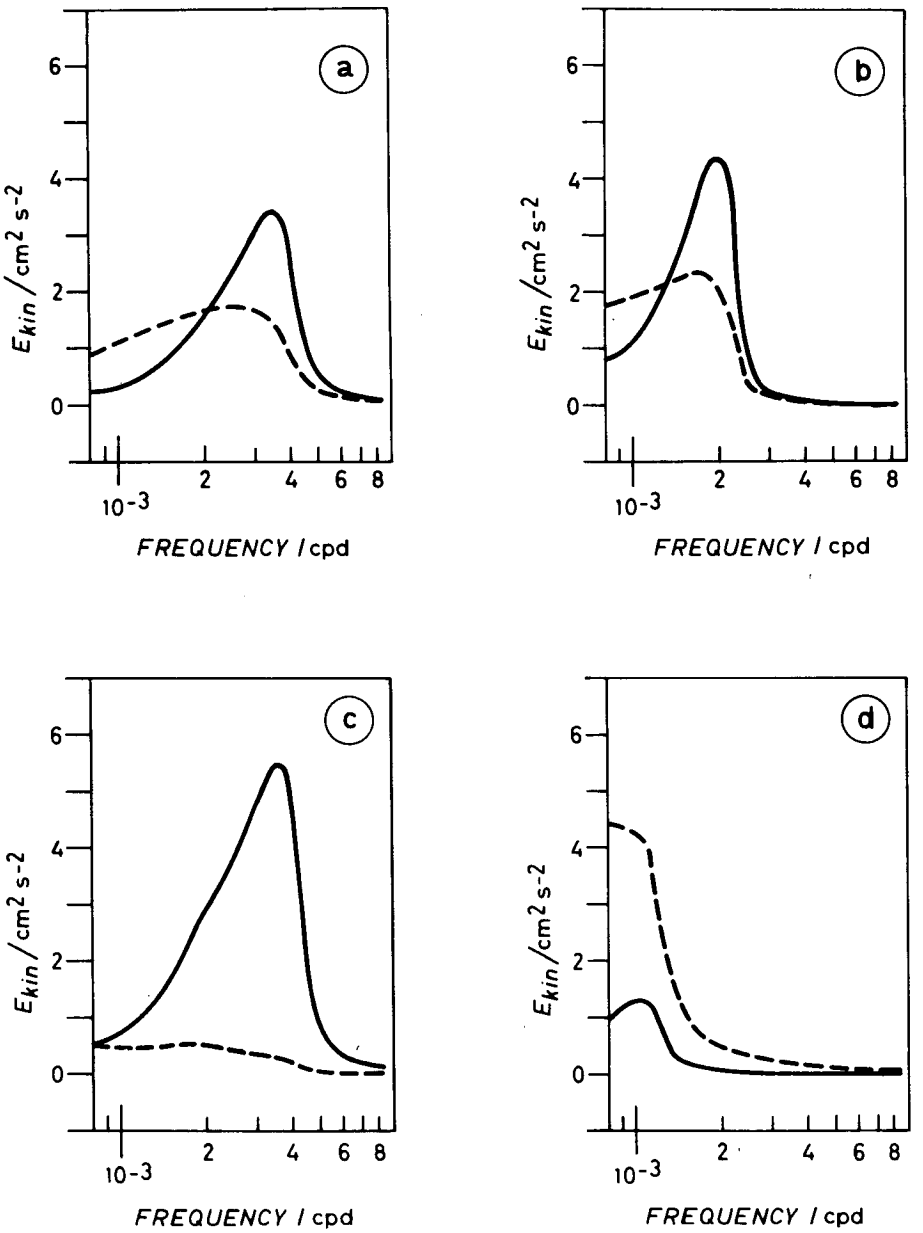

FIG. 5. Frequency spectra of meridional (solid line) and zonal component (dashed line) of kinetic energy generated by different wavenumber bands of the windstress curl. (a) $\kappa_b = \eta_b = 2\pi/5000$ km, $\kappa_c = \eta_c = 2\pi/500$ km; (b) $\kappa_b = \eta_b = 2\pi/5000$ km, $\kappa_c = \eta_c = 2\pi/3000$ km; (c) $\kappa_b = \eta_b = 2\pi/5000$ km, $\kappa_c = 2\pi/3000$ km, $\eta_c = 2\pi/500$ km; (d) $\kappa_b = \eta_b = 2\pi/5000$ km, $\kappa_c = 2\pi/500$ km, $\eta_c = 2\pi/3000$ km.

$$\left.\begin{aligned}
\Omega_{\text{pot}}(\omega, \eta, x, z) &= \int_{-\infty}^{+\infty} \sum_{n=1}^{\infty} f_0^2 \lambda_n^2 Z_n^2|_{z=0} |R|^{-2}(1 + e^{-2\kappa_i X} - 2\cos\alpha e^{-\kappa_i X}) d\kappa \\
\Omega_u(\omega, \eta, x, z) &= \eta^2 \int_{-\infty}^{+\infty} \sum_{n=1}^{\infty} Z_n^2|_{z=0} |R|^{-2}(1 + e^{-2\kappa_i X} - 2\cos\alpha e^{-\kappa_i X}) d\kappa \\
\Omega_v(\omega, \eta, x, z) &= \int_{-\infty}^{+\infty} \sum_{n=1}^{\infty} Z_n^2|_{z=0} |R|^{-2}(\kappa^2 - 2\kappa(\kappa_r \cos\alpha + \kappa_i \sin\alpha) e^{-\kappa_i X}) + (\kappa_r^2 + \kappa_i^2) e^{-2\kappa_i X}) d\kappa
\end{aligned}\right\} \quad (17)$$

with real and imaginary part of the wavenumber according to

$$\kappa_n = \kappa_r + i\kappa_i = \left(1 + \frac{i\mu_0 N_0^2 \lambda_n^2}{\omega}\right)^{1}\left\{\frac{\beta}{2\omega} - \left[\frac{\beta^2}{4\omega^2} - \eta^2\left(1 + \frac{i\mu_0 N_0^2 \lambda_n^2}{\omega}\right)^{-2} - f_0^2 \lambda_n^2 \left(1 + \frac{i\mu_0 N_0^2 \lambda_n^2}{\omega}\right)^{-1}\right]^{1/2}\right\}$$

and $\alpha = \kappa - \kappa_n$.

The energy spectra are not homogeneous in space. Due to the fixed phase required to fit the boundary condition at the eastern coast, they depend on the actual distance to the shore. Thus, we recognize two different dynamical regions. Near the coast the directly forced waves are superimposed on the waves generated at the coast. Far away from the coast ($x \rightarrow \infty$) the contributions of the westward propagating waves generated at the coast vanish, since the energy is dissipated on its way. In that region the energy distribution is homogeneous and the resulting spectrum resembles the MF-spectrum.

b. *Zero-wavenumber forcing*

White's (1977) solution is a special case of (16) which he obtained by prescribing a curl wavenumber spectrum concentrated at zero wavenumber and by neglecting friction. It is remarkable that the inclusion of an eastern boundary allows the generation of waves which have completely different scales than the forcing spectrum. Since White uses a two-layer model, his solution corresponds to the first mode only. It is interesting to note that in this case the potential energy is related to the meridional kinetic energy by

$$E_{\text{pot}}(\omega)/E_{\text{kin}}(\omega) = (4\omega_c/\omega)^2 \sin^2[\omega x/(2c_1)] \quad (18)$$

with

$$E_{\text{kin}}(\omega) = F_{\text{rot}\tau}(\omega)/(H\beta^2), \quad (19)$$

where H is the water depth in the case of constant Väisälä frequency. Thus, the potential energy contains a modulation factor whereas the kinetic energy is homogeneous. This criterion could be used to distinguish between direct and coastal forcing.

Since ω_c/ω is always larger than unity, the potential energy is at least 8 times the horizontally averaged kinetic energy. The ratio increases rapidly with smaller frequencies.

If the forcing is made up by a single peak in the frequency range, e.g., the annual frequency, the potential energy of the first mode baroclinic waves in the White model shows a sine-square longitudinal dependence. Maxima and minima of potential energy alternate with a wavelength that is two times the wavelength of free waves, $L = 8\pi r_1 \omega_c/\omega$. For the annual cycle we find $L = 700$ km for a baroclinic cutoff period of ½ year and $\beta = 2.0 \times 10^{-13}$ s^{-1}. Waves caused by this mechanism must show significant changes in the potential energy as a function of distance to the eastern coast.

In Magaard's (1983) review the spectra of first mode baroclinic Rossby waves reveal a broad band around the annual frequency. Thus, the model requires a broad band forcing in the frequency range. Figure 6 displays the frequency spectra of the vertically integrated potential energy as a function of distance from the coast for a white-noise frequency spectrum of the forcing, calculated after equation (17) with $\kappa = \eta = 0$.

There is a small amount of potential energy in the vicinity of the eastern coast. Due to the modulation by the sine-square term, there are maxima at frequencies $\omega = 0$; $\omega_{\max} = 4(2m - 1)\pi r_1 \omega_c/x$ as long as ω is smaller than ω_c. Therefore, there is no maximum in the frequency range between 0.1 and 2 cpy within 2π Rossby radii. The spectrum shows a monotonic decrease according to $A_0\{1 - \frac{1}{3}[\omega x/(4r_1\omega_c)]^2\}$. Strictly speaking, the solution is not applicable at very low frequencies because they are within the time-scale of the general circulation which is not adequately described by this simple linear model.

Since the low-frequency Rossby waves ($\omega \leq 0.1$ cpy) have wavelengths of ocean basin dimension, the propagating wave model does not hold. The essential characteristics of this linear model are the tendency of increasing potential energy with increasing distance in the range $\omega \leq 1$ cpy and the formation of several spectral maxima. The total variance in a given frequency band is dominated by long waves due to the fact that the energy is strongly concentrated at low frequencies. The consequence of the zero wavenumber forcing is a purely westward phase propagation and a nonrandom phase coupling.

c. *Nonzero-wavenumber forcing*

A different form of the energy spectrum is obtained if the windstress curl has a zonal length scale which

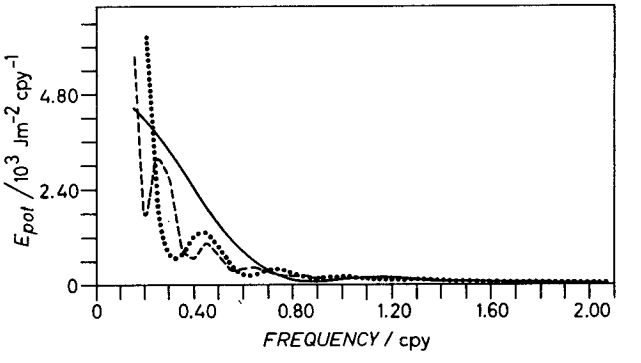

FIG. 6. Frequency spectra of potential energy at different distances from the eastern boundary (solid line: 1000 km, dotted line: 3000 km, dashed line: 5000 km).

is considerably smaller than the basin width. In the following we calculate the corresponding spectra with a wavenumber spectrum of the form (12). In this case resonant forcing is possible and friction is necessary to prevent infinitely large response for stationary stochastic forcing. The use of friction also implies that the coastally forced waves damp out and that the spectrum approaches the directly forced ones far from the coast. This is shown in Fig. 7 where we display potential (a), zonal (b) and meridional (c) depth-integrated first mode energy spectra. The forcing is restricted to a range of scales of 5000 and 500 km. Thus, contrary to the zero wavenumber case, phase propagation is not purely zonal. In fact, all wavenumbers between (κ_c, η_b) and (κ_b, η_c) are feasible. The bulk of the energy is concentrated at frequencies of 0.2–1.6 cpy. The increase of the energy level and the tendency to adjust to the directly forced spectrum is more pronounced at higher frequencies. Therefore, the range with maximum energy broadens at large separations due to selective damping by virtual friction which reduces the energy of the higher wavenumber components more rapidly. The e-folding distance of free dispersive waves, which in the nondispersive range can be approximated by

$$X = \frac{\beta^3 r_1^4}{2\omega^2 R}, \qquad (20)$$

is shown in Fig. 8 for three different values of R. Typical distances at $\omega = 1$ cpy are 2500, 1200 and 320 km for $R = 5.55 \times 10^{-8}$, 1.11×10^{-7} and 5.55×10^{-7} cm^2 s^{-1}, respectively.

If we used MF-damping, all frequencies were equally damped. Thus, the directly forced spectrum would be achieved within a distance of one Rossby radius off the coast using 200 days damping time according to MF. In the nonfriction case, no stationary spectrum can be achieved and the energy spectrum increases continuously with distance.

Thus, by choosing a specific frictional damping we fix the range where an equilibrium spectrum is possible. The form of the spectrum in the non-equilibrium range is not strongly dependent on the magnitude of the friction. Using our damping, the total energy does not differ much from the frictionless case within several thousands of kilometers.

A further question of interest is the fractional content of energy in the individual modes. The contribution of the higher modes is more pronounced in the potential energy spectra depending on frequency.

The contributions of the higher modes to potential energy are less than 2% of that of the first mode at $\omega = 1$ cpy; but at $\omega = 0.3$ cpy they are in the order of the first mode near the coast and about 10% at a distance of 5000 km. Thus, in the spectral band of 0.5–2.0 cpy, there is an obvious dominance of the first mode. But the influence of higher modes increases

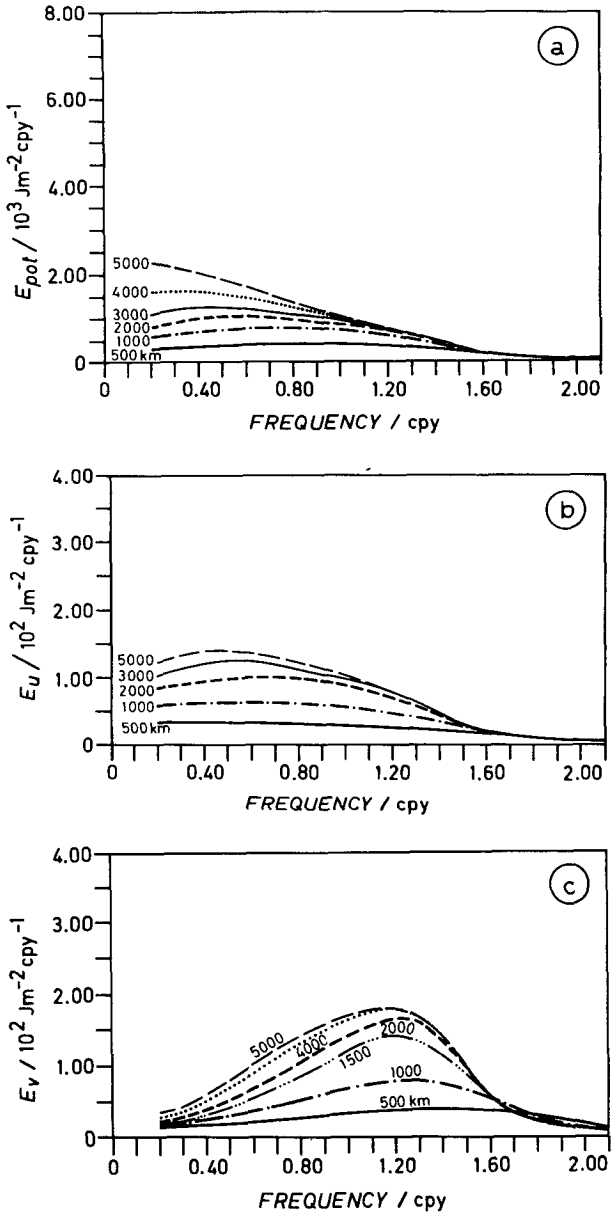

FIG. 7. Frequency spectra of potential energy (a), zonal (b) and meridional component (c) of kinetic energy at different distances from the eastern boundary.

at lower frequencies. Also, the effect of the higher modes is even stronger in the actual depth-dependent spectra and is weighted towards small depths. This is due to the deterministic coupling of the individual modes which in our model—contrary to MF—is not based on statistically independent vertical modes. The result of this coupling is the destructive interference at larger depths and the accumulation of high mode energy in the near-surface region. Furthermore, the high modes are of greater importance in the vicinity of the coast where the spectrum converges to its limiting form at small distances. Finally, the zero-

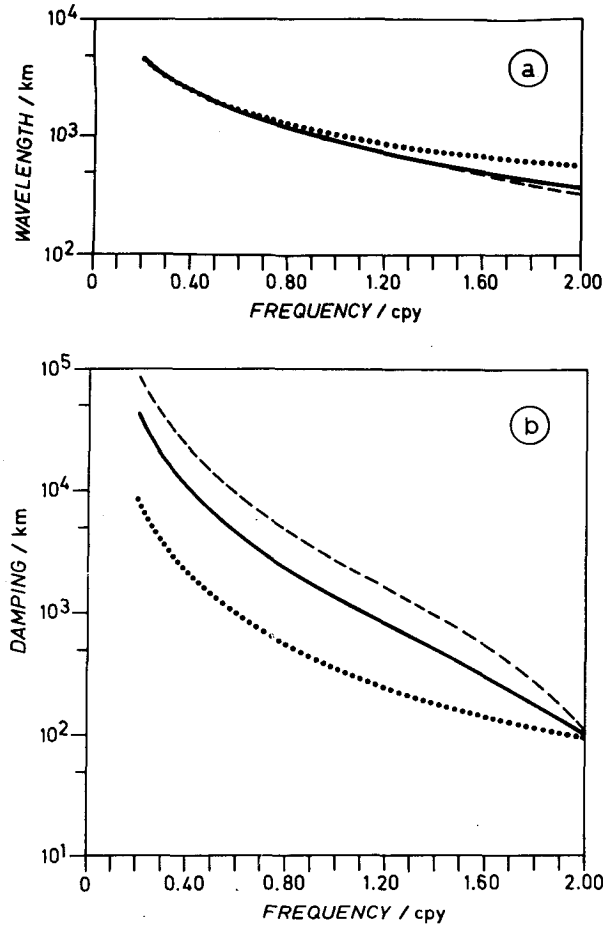

FIG. 8. Real part (a) and imaginary part (b) of the resonant wavenumber with different damping; solid line: $R = 1.11 \times 10^{-7}$ s^{-1}, dashed line: $R = 5.55 \times 10^{-8}$ s^{-1}, dotted line: $R = 5.55 \times 10^{-7}$ s^{-1}.

forcing case is an integral part of the nonzero case if the zonal wavenumber is within the range $0 \leqslant \kappa \ll \omega/(2\omega_c r_1)$.

5. Discussion

The model presented in the previous chapters was designed to investigate the influence of different windstress curl wavenumber spectra on the direct forcing of baroclinic Rossby waves and modifications due to the presence of an eastern boundary.

Focussing on the direct forcing we demonstrated that in agreement with an earlier model (MF) a bandlimited white-noise frequency and wavenumber spectrum of the curl-forcing leads to an equivalent white-noise kinetic energy spectrum in the frequency range of baroclinic Rossby waves ($\omega \leqslant \omega_c$, Eq. 13). Gallegos-Garcia *et al.* (1981) presented evidence of white curl spectra in the transition region between the Pacific Westerlies and the Northeast Trades. There is little doubt that the frequency spectrum of windstress curl is flat at frequencies $\omega \leqslant \omega_c$, whereas the wavenumber structure is less established. It was, therefore, worthwhile to consider cutoff wavenumbers in a hypothetical curl spectrum which differ from those suggested by MF. The consequence of a reduced bandwidth due to a larger scale curl is a shift of the response cutoff frequency to values $\omega \leqslant \omega_c$ if the largest zonal wavenumber of the forcing (κ_c) is smaller than the inverse Rossby radius of the first baroclinic mode. Thus, the range of resonantly excited waves is reduced. This also holds if the scale of the forcing is diminished as expressed by a larger value of the low wavenumber limit k_b (cf. Figs. 3 and 4). In order to clarify the influences of the different bandlimits k_b and k_c, the cutoffs in our calculations were infinitely sharp. Real spectra with a moderate falloff beyond the bandlimits do not produce a completely different response if most of the variance in the curl field is contained in the white-noise range. The main result concerning the directly forced response in the range of resonant baroclinic waves is the band structure of the kinetic energy around the annual period which is to be considered as a consequence of the curl band structure in the wavenumber space although the frequency spectrum of the forcing is essentially white in this range.

At first glance it seems a bit artificial to explain the generation of annual waves by the bandlimitation of a white-noise windstress curl, while the actual annual peak in the forcing is neglected. Due to the linearity of the model the inclusion of an annual peak would just enhance the energy content around the annual band depending on the magnitude of the peak. But data analysed by Gallegos-Garcia *et al.* (1981) show no significant peaks in this range at the 90% level.

The model extension which took account of a meridional eastern boundary revealed that the homogeneous spectrum of the directly forced response in an infinite ocean is the limiting form at large distances. Friction determines the range beyond which the response tends to its homogeneous form. In order to justify the use of a model which ignores lateral boundaries, particularly strong damping is required (see Fig. 8). For less damped waves the spectra are inhomogeneous in the range exceeding the size of realistic oceans. Consequently, there is a monotonic increase in baroclinic Rossby wave energy off the eastern boundary, and the magnitude of the directly forced spectrum is the upper limit of the response.

There are several characteristics which classify the two different dynamical regions. First, the near coast region is dominated by the propagation of long (but not generally dispersion-free) baroclinic first mode waves which balance the surplus of zonal momentum by the nonresonant forced part and the short, resonantly excited waves at the eastern boundary. Thus, with a stochastic forcing model, the structure of the

response at a given frequency is not much different from that obtained with a deterministic model in this dynamical region. This was confirmed by comparing amplitudes and phases of a local cosine-fit performed upon realizations of our model and that of White and Saur (1981). The dominant wavelength can be inferred from the first mode dispersion-relation which—also by its imaginary part—determines the separation between the two dynamical regions. Secondly, in the far-away field the response is dominated by the resonantly generated long baroclinic waves. The magnitude of the spectrum as well as the mean wavelength depend on the distribution of the curl wavenumber spectrum. It follows that a model, as suggested here, can resolve the discrepancy in the interpretation of Rossby wave data by Price and Magaard (1983) and White and Saur (1981). Such a model can also explain the existence of a broad energy maximum around the annual frequency even if there is no pronounced peak in the forcing. In addition, we find that with increasing distance from the coast the band broadens as observed by Magaard (1983).

It should be pointed out again that the main restriction of the stochastic stationary forcing model is the requirement of damping which determines both the mean energy level and the scale of the near and the far field. In a relatively "narrow ocean" (e.g., the Atlantic), a far field does not exist for long relaxation times. Even with the damping in our examples, the influence of the eastern boundary is obvious even in the vicinity of a western boundary if the frequency is smaller than 0.5 cpy. On the other hand, the influence of the western boundary is limited to a much shorter

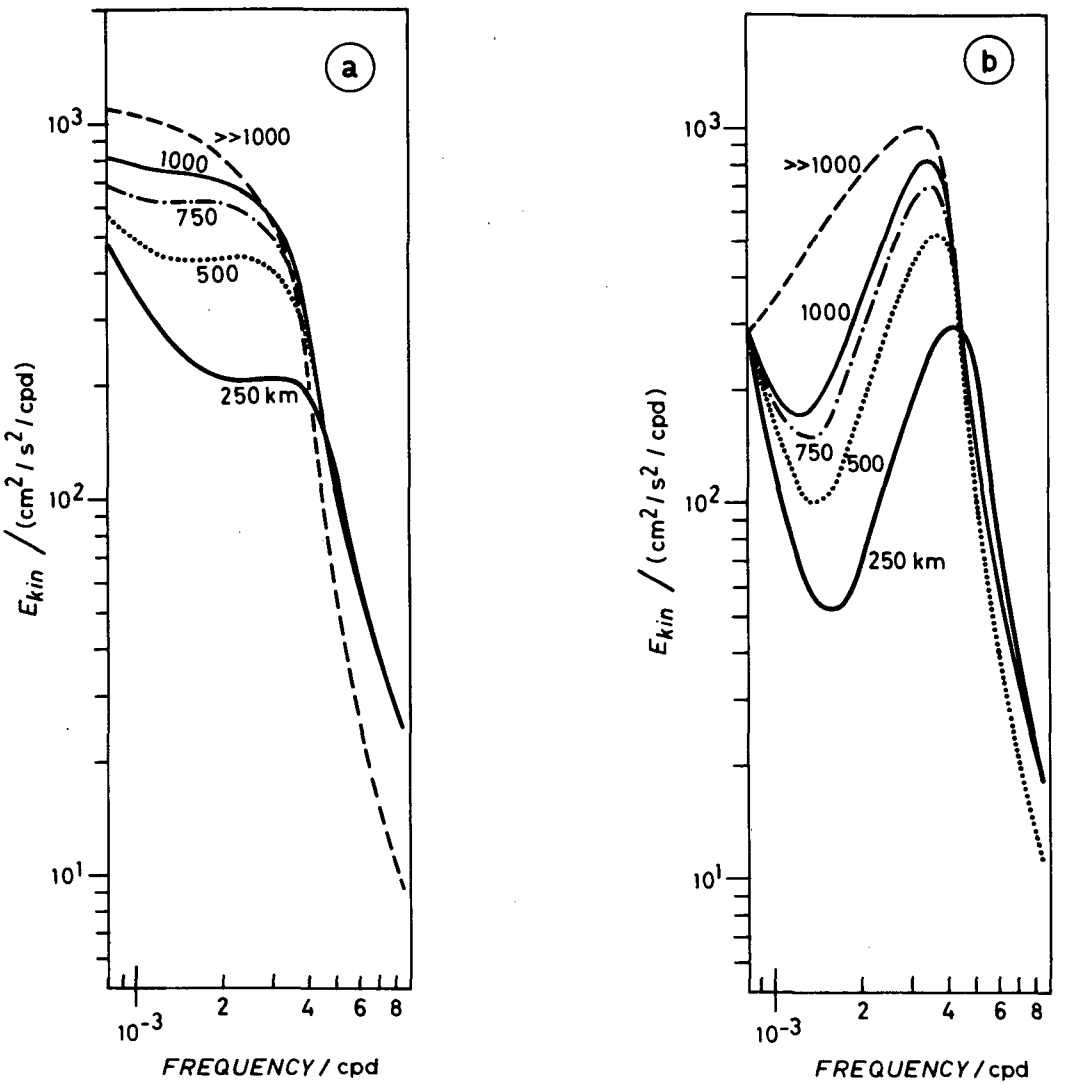

FIG. 9. Frequency spectra of zonal (a) and meridional (b) kinetic energy generated by a broad band forcing at different distances from the eastern boundary and the homogeneous spectrum in the far field.

range. This is due to the fact that the long waves are transformed to short ones after reflection and are essentially damped out on a scale that corresponds to the western boundary current. The eastern boundary, therefore, plays the dominant role for the dynamics in the midocean and eastern basins. Comparing measured spectra outside the western boundary with theoretical Rossby wave models seems to be useful only when the influence of the eastern boundary is incorporated. Even if the Mid-Atlantic Ridge were a blocking boundary at all depths, the one-sided model including the eastern boundary would be appropriate in most parts of the eastern basins. As an example, Fig. 9 exhibits zonal and meridional kinetic energy spectra at several distances from the coast. The increase of energy with distance is well established. The same is valid for the more pronounced band structure in the meridional component. However, the variance in both components is not essentially different from one another, and the observed anisotropy in the Canary Basin (see Fig. 1) is not revealed in the case of broad band forcing. The result is different for a narrow band forcing which leads to a significant higher energy level of the meridional component (see Section 3).

The zonal distribution of Rossby wave energy is fairly well known in the Pacific. In the Atlantic Ocean, a ship-of-opportunity XBT-Program has been organized (Dobson *et al.*, 1982) which will improve the data base. J. M. Price (personal communication, 1983) is presently examining the NODC data set and concentrates his studies on first mode energy like the analysis made with respect to the Pacific.

A step forward in modeling, however, requires a detailed knowledge of the spectral distribution of the windstress curl on scales of the first mode Rossby radius, information which will hopefully be provided by satellite winds in the near future.

REFERENCES

Anderson, D. L. T., and A. E. Gill, 1975: Spin-up of a stratified ocean with applications to upwelling. *Deep-Sea Res.*, **22**, 683–696.

Broecker, W. S., 1981: Geochemical tracers and ocean circulation. *Evolution of Physical Oceanography*, B. A. Warren and C. Wunsch, Eds., MIT Press, 140–183 pp.

Dobson, F. E., F. P. Bretherton, D. M. Burridge, J. Crease, E. B. Kraus and T. H. von der Haar, 1982: The CAGE experiment: A feasibility assessment report. WCP Report Series No. 22. World Meteorological Organization, Geneva.

Fjeldstad, J. E., 1964: Internal waves of tidal origin. Part 1: Theory and analysis of observations. *Geophys. Publ.*, **25**(5), 1–73 pp.

Frankignoul, C., and P. Müller, 1979: Quasi-geostrophic response of an infinite β-plane ocean to stochastic forcing by the atmosphere. *J. Phys. Oceanogr.*, **9**, 104–127.

Gallegos-Garcia, A., W. J. Emery, R. O. Reid and L. Magaard, 1981: Frequency-wavenumber spectra of sea surface temperature and wind-stress curl in the Eastern Pacific. *J. Phys. Oceanogr.*, **11**, 1059–1077.

Kang, Y. Q., and L. Magaard, 1980: Annual baroclinic Rossby waves in the central North Pacific. *J. Phys. Oceanogr.*, **10**, 1159–1167.

Käse, R. H., and C. L. Tang, 1976: Spectra and coherence of wind-generated internal waves. *J. Fish. Res. Board Can.*, **33**(10), 2323–2328.

——, W. Zenk, T. B. Sanford and W. Hiller, 1984: Currents, fronts and eddy fluxes in the Canary Basin. *Progress in Oceanography*, Pergamon, (in press).

Krauss, W., and C. Wübber, 1981: Response of the North Atlantic to annual wind variations along the eastern coast. *Deep Sea Res.*, **29**, 851–868.

Magaard, L., 1977: On the generation of baroclinic Rossby waves in the ocean by meteorological forces. *J. Phys. Oceanogr.*, **7**, 359–364.

——, 1983: On the potential energy of baroclinic Rossby waves in the North Pacific. *J. Phys. Oceanogr.*, **13**, 38–42.

McCreary, J. P., 1981a: A linear stratified ocean model of the Equatorial Undercurrent. *Phil. Trans. Roy. Soc.*, **A298**, 603–635 pp.

——, 1981b: A linear stratified ocean model of the coastal undercurrent. *Phil. Trans. Roy. Soc.*, **A302**, 385–413 pp.

Müller, P., and C. Frankignoul, 1981: Direct atmospheric forcing of geostrophic eddies. *J. Phys. Oceanogr.*, **11**, 287–308.

Mysak, L. A., 1983: Generation of annual Rossby waves in the North Pacific. *J. Phys. Oceanogr.*, **13**, 1908–1923.

——, and L. Magaard, 1983: Rossby wave driven eulerian mean flows along non-zonal barriers with application to the Hawaiian Ridge. *J. Phys. Oceanogr.*, **13**, 1716–1725.

Price, J. M., and L. Magaard, 1983: Rossby wave analysis of subsurface temperature fluctuations along the Honolulu–San Francisco Great Circle. *J. Phys. Oceanogr.*, **13**, 258–268.

Veronis, G., 1981: Dynamics of large-scale ocean circulation. *Evolution of Physical Oceanography*, B. A. Warren and C. Wunsch, Eds., MIT Press, 140–183 pp.

——, and H. Stommel, 1956: The action of variable wind-stresses on a stratified ocean. *J. Mar. Res.*, **15**, 43–75.

White, W. B., 1977: Annual forcing of baroclinic long waves in the tropical North Pacific. *J. Phys. Oceanogr.*, **7**, 50–61.

——, and J. F. T. Saur, 1981: A source of annual baroclinic waves in the Eastern Subtropical North Pacific. *J. Phys. Oceanogr.*, **11**, 1452–1462.

Willebrand, J., 1981: Zur Erzeugung großräumiger ozeanischer Strömungsschwankungen in mittleren Breiten durch veränderliche Windfelder. Berichte aus dem Institut f. Meereskunde Kiel Nr. 83.

——, S. G. H. Philander and R. C. Pacanowski, 1980: The oceanic response to large-scale atmospheric disturbances. *J. Phys. Oceanogr.*, **10**, 411–429.